文章编号:1001-9014(2007)01-0001-04

BEHAVIOR OF Si INCORPORATION IN $Al_x Ga_{1-x} As$ ($x = 0$ TO 1) GROWN BY GAS SOURCE MOLECULAR BEAM EPITAXY

LI Hua[1], LI Ai-Zhen[1,2], ZHANG Yong-Gang[1], QI Ming[1]

(1. State Key Laboratory of Functional Materials for Informatics, Shanghai Institute of Microsystem and Information Technology, Chinese Academy of Sciences, Shanghai 200050, China;
2. East China Normal University, Shanghai 200062, China)

Abstract: The doping behavior of Si in AlGaAs with AlAs mole fraction from 0 to 1 was reported. Si-doped $Al_xGa_{1-x}As$ layers were grown by gas source molecular beam epitaxy with a constant Si cell temperature for all samples. The electrical properties and composition of the ternary alloys were characterized by Hall effect and X-ray diffraction, respectively. Results show that the electron concentration of Si-doped $Al_xGa_{1-x}As$ varying with Al mole fraction has a minimum value at x = 0.38, which is the Γ-X direct-indirect band crossover of AlGaAs system. The Hall mobility decreases with the increasing of AlAs mole fraction till about x = 0.4, hereafter it remains at a low value of mobility with small change rate.

Key words: gas source molecular beam epitaxy; $Al_xGa_{1-x}As$; Si-doped; electrical properties; composition
CLC number: **Document**: A

气态源分子束外延 $Al_x Ga_{1-x} As$($x = 0 \sim 1$)材料中Si的掺杂行为研究

李 华[1], 李爱珍[1,2], 张永刚[1], 齐 鸣[1]

(1. 中国科学院上海微系统与信息技术研究所,信息功能材料国家重点实验室,上海 200050;
2. 华东师范大学信息学院,上海 200062)

摘要:研究了Si在$Al_xGa_{1-x}As(0 \leqslant x \leqslant 1)$中的掺杂行为.为比较Al组份对Si掺杂浓度的影响,在用气态源分子束外延生长(GSMBE)掺Si n型$Al_xGa_{1-x}As(0 \leqslant x \leqslant 1)$的所有样品时,n型掺杂剂Si炉的温度恒定不变.用Hall效应测量外延层的自由载流子浓度和迁移率,用X射线双晶衍射迴摆曲线测量外延层的组份.测试结果表明,当$Al_xGa_{1-x}As$中Al组份从0增至0.38时,Si的掺杂浓度从4×10^{18} cm^{-3}降至7.8×10^{16} cm^{-3},电子迁移率从1900 cm^2/Vs降至100 cm^2/Vs.这与$Al_xGa_{1-x}As$材料的Γ-X直接—间接带隙的转换点十分吻合.在$Al_xGa_{1-x}As$全组份范围内,自由载流子浓度随Al组份从0至1呈"V"形变化,在X = 0.38处呈最低点.在x > 0.4之后,$Al_xGa_{1-x}As$的电子迁移随Al组分的增加,一直维持较低值且波动幅度很小.

关 键 词:气态源分子束外延;AlGaAs;Si掺杂;电学性质;组分

Introduction

AlGaAs is the most studied and the most widely used Ⅲ-V semiconductor. Binary GaAs and AlAs are almost lattice matched, so AlGaAs ternary alloy is quite suitable for epitaxial growth on GaAs substrate and is widely used in optoelectronic and high-speed electronic devices. Applications require high quality n-

Received date: 2006-07-31, **revised date**: 2006-10-20 **收稿日期**:2006-07-31,**修回日期**:2006-10-20
Foundation Item: Supported by the National Natural Science Foundation of China (60136010, 60676026, 60406008), National 973 Project of China (2006CB604903)
Biography: LI Hua (1979-), male, Jiangsu, China. Candidate for Doctor degree. Research area is semiconductor optoelectronic materials and devices.

type AlGaAs, which can be obtained by doping with group IV elements Si, Sn or group VI ones Se, Te. Among them, Si acts as a nearly ideal n-type dopant for MBE grown AlGaAs materials. An abnormal donor doping variation with Al composition has been observed in various n-type dopants for AlGaAs grown by different growth techniques such as solid source MBE, MOCVD and LPE. Ishibashi et al [1,2] observed that the carrier concentration in Si-doped AlGaAs decreased and reached a minimum value at x = 0.34, simultaneously the donor ionization energy E_D increased abruptly to a maximum value of 150meV at $x = 0.36$[1]. He also reported that the ionization energy reached a maximum value at $x = 0.37$ in the composition region $0 \leqslant x \leqslant 0.5$[2]. Chand et al. [3] reported that a shallow donor level ($\leqslant$15meV) tied to the Γ band and a deep donor level tied to the L band was dominant for $x > 0.2$, and reached the peak at 160meV for $x \sim 0.4$. The abnormal variation was also observed in Te-doped AlGaAs and interpreted by Lang et al. [4] with so-called *DX* centers, which were also investigated in Sn-doped AlGaAs. [5] Watanabe et al. [6,7] suggested that the abnormal donor ionization energy obtained from Hall measurement was mainly due to the change in the concentration ratio of shallow donor centers and *DX* centers. There have been detailed investigations on Si-doped AlGaAs both theoretically and experimentally, however, all studies were based on tetrameric As_4 source or solid dimeric As_2 source, and have never been demonstrated on gas source molecular beam epitaxy (GSMBE) systems with cracked arsine source. As well know that Aluminium is a very active element, therefore, very easier to react with oxygen to form an Al_xO_y layer on the surface. Comparison of GSMBE and SSMBE, first, GSMBE could provide a hydrogen reduction ambient during cracking arsine (AsH_3) to suppress Al_xO_y layer ; second, the deep level impurity in $Al_xGa_{1-x}As$ are depended on the As species, the deep level impurity in AlGaAs growing from As_2 source is much less than growing from As_4. GSMBE uses arsine as a group V source, while AsH_3 cracking at high temperature, the AsH_3 will be entirely cracked into As_2 (>99). GSMBE has advantages [8,9], in particularly for Al-based compounds.

In this paper, we report a detailed study on the doping behavior of $Al_xGa_{1-x}As$ grown by GSMBE, particularly concentrating on the electrical properties of Si-doped $Al_xGa_{1-x}As$ layers covering the entire composition range ($x = 0$ to 1).

1 Experimental procedure

The MBE system employed in this study was a V80H gas source MBE system. 6N AsH_3, 6N Al and 6N Ga were used as the source of group V and group Ⅲ, respectively. A thermo-cell with a two zone heater was used as gallium cell to impede gallium droplet forming, which can reduce the oval defects efficiently. In every experiment, a quarter of 2-inch Epi-ready (100)-oriented un-doped semi-insulating GaAs substrate was mounted on a molybdenum ring holder with a quarter of 2-inch hollow. Reflection high energy electron diffraction (RHEED) was located in the growth chamber to monitor the surface cleaning treatment. Prior to growth, the substrate was heated to 300℃ in the preparation chamber to desorb water and carbon dioxide on the surface for preventing contamination of the deposition chamber. Then the substrate was transferred to the growth chamber and heated up in the presence of ambient arsenic till the surface oxides were desorbed under the monitor of RHEED. The growth temperature was 50℃ lower than the desorption temperature. The temperature was measured by a W-Re thermocouple. During growth, the substrate was rotated with a rotation speed of 10 rounds per minute to ensure uniform flux distribution which related to composition and thickness uniformity of epilayer. The arsine was cracked to dimeric As_2 at 1000℃ by a high pressure cracker. The pressure during layer growth was set to be 2×10^{-5}Torr in the deposition chamber. In order to obtain a desired constant Si doping flux for comparison the effect of Al mole fraction on donor level, the Si-cell temperature was fixed at 1200℃ during GSMBE growth for all samples.

After growth, the alloy composition of all samples was characterized by a Philips X'Pert high resolution double-crystal X-ray diffractometer with a Cu $K\alpha_1$ radiation source and a Ge fourfold monochrometer. (0 0 4) reflections were measured with the high voltage at

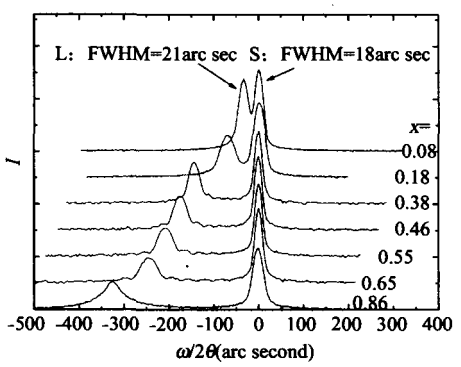

Fig. 1 Double crystal X-ray diffraction rocking curves of $Al_xGa_{1-x}As$ layers with variation Al mole fraction. The FWHM values for the epilayer (L) with AlAs mole fraction of 0.08 is 21arcsec, and the GaAs substrate (S) of 18 arcsec
图 1 不同 Al 组分的 $Al_xGa_{1-x}As$ 外延层的双晶 X 射线衍射摇摆曲线. 图中 AlAs 摩尔组分为 0.08 的外延层衍射峰(L)的半高宽为 21 弧秒, 相应的衬底峰(S)半高宽为 18 弧秒. 纵坐标 I 代表强度

30kV and the current at 15mA for all the layers. Due to the lattice mismatch between AlGaAs layer and GaAs substrate is in the order of 10^{-3}, the measurement of full strained composition value was chosen as the composition in this study. An AMBIOS XP-2 high resolution surface profilometer was employed to measure the thickness of the layers. The Van der Pauw technique was used to characterize the electrical properties of the AlGaAs layers at room temperature though a GPIB controlled Hall-effect equipment, and the ohmic contacts were formed by alloying indium dots.

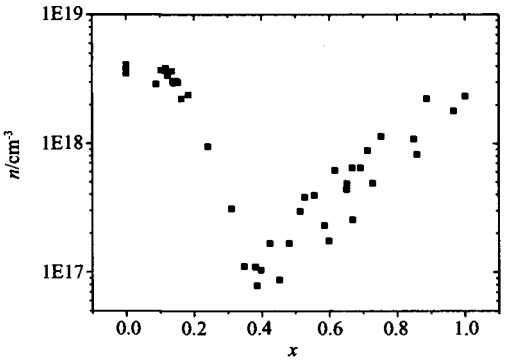

Fig. 2 Free electron concentrationn versus Al compositionx at room temperature for Si-doped $Al_xGa_{1-x}As$ ($x=0$ to 1). The temperature of Si donor dopant is kept at 1200℃ for all $Al_xGa_{1-x}As$ ($x=0$ to 1) samples. It is clearly shown that the electron concentration versus Al mole fraction exhibits an italic "V" shape. The electron concentration dropped from 4×10^{18} cm^{-3} (AlAs = 0) to $7.8\times10^{16}cm^{-3}$ (AlAs = 0.38)
图 2 室温下掺 Si n 型 $Al_xGa_{1-x}As$ ($x=0$ to 1)外延层的自由载流子浓度 n 与 Al 组份 x 的关系. GsMBE 生长所有不同组份的外延层时, Si 炉温度恒定为 1200℃. 图 2 显示载流子浓度随 Al 组分的变化呈明显的"V"形走势. 当 Al 组份从 0 增至 0.38 时, 自由电子浓度从 $4\times10^{18}cm^{-3}$ 降至 $7.8\times10^{16}cm^{-3}$

2 Results and discussions

X-ray diffraction rocking curve is measured on every AlGaAs layers, as shown in Fig. 1. The full-width at half-maximum (FWHM) of all epilayers is between 21arcsec and 38arcsec, and the FWHM of substrates is about 18arcsec. From Fig. 1, it could be seen that, with the increase of the AlAs mole fraction, the FWHM of the epilayer also increases slightly. However, it still keeps at a quite low level, indicating excellent single crystal quality and uniformity in the whole AlAs mole fraction range.

Hall free-carrier concentration of Si-doped $Al_xGa_{1-x}As$ epilayers at room temperature as a function of AlAs mole fraction were shown in Fig. 2. From Fig. 2, it was clearly exhibited that at the same Si doping flux, the electron concentration decreases dramatically from $4\ 10^{18}\ cm^{-3}$ to $7.8\ 10^{16}\ cm^{-3}$, while the AlAs mole fraction x increases from 0.1 to about 0.4, then rises slowly until $x=1$. Fig. 3 shows the variation of electron mobility with alloy composition measured. The mobility decreases with increasing AlAs mole fraction of $0<x<$

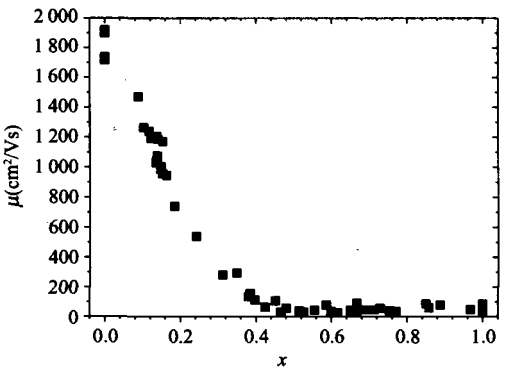

Fig. 3 Hall electron mobility M for Si-doped n-type $Al_xGa_{1-x}As$ versus AlAs mole fraction x at 300 K. The mobility decreases from 1900 cm^2/Vs to 100 cm^2/Vs with the increasing of AlAs mole fraction from 0 to 0.38, and thereafter, remains at low value around 50 cm^2/Vs with little fluctuation till $x=1$
图 3 Si 掺杂 n-型 $Al_xGa_{1-x}As$ 材料的 Hall 迁移率 M 随 Al 组分 x 的变化. 在 $0<x<0.4$ 区间内, 随 AlAs 组分的增加, 迁移率从 1900 cm^2/Vs 降到 100 cm^2/Vs; $x>0.4$ 时, 其迁移率维持在 50 cm^2/Vs 左右, 变化幅度很小

0.4. And for $x > 0.4$, the Hall electron mobility remains low in $Al_xGa_{1-x}As$ layers. It is noticeable that the electron mobility only changes slightly and independent of AlAs mole fraction when $x > 0.45$, where the Hall electron nobilities are between $30cm^2/Vs$ and $60cm^2/Vs$.

Table 1 Bandgap structure parameters[10] and bowing parameters[11] used in Fig. 4

表1 图4中采用的GaAs, AlAs能带结构参数[10]和弯曲系数[11]

Bandgaps	Bowing parameter C	E_g of GaAs (eV)	E_g of AlAs (eV)
Γ valley	0.37	1.519	3.099
X valley	0.144	1.981	2.24
L valley	0	1.815	2.46

To understand the drop of electron concentration in Fig. 2, the composition dependences for the direct and indirect gaps in $Al_xGa_{1-x}As$ were plotted in Fig. 4. For AlGaAs alloy, the dependence of energy gap on alloy composition is assumed to fit a simple quadratic form [10]

$$E_g(AL_xGa_{1-x}As) = xE_g(AlAs) + (1-x)E_g(GaAs) - x(1-x)C \quad , (1)$$

where the bowing parameter C accounts for the deviation from a linear interpolation between two binaries AlAs and GaAs. The recommended values of the nonzero bowing parameters[11] and the bandgap structure parameters[10] of both binaries used in this study are listed in Table 1. The crossover points are: $x(L\text{-}X) = 0.35$, $E_L = E_X = 2.04eV$, $x(\Gamma\text{-}X) = 0.39$, $E_\Gamma = E_X = 2.05eV$, $x(\Gamma\text{-}L) = 0.41$, $E_\Gamma = E_L = 2.08eV$. And the direct-indirect bandgap crossover is at $x = 0.39$.

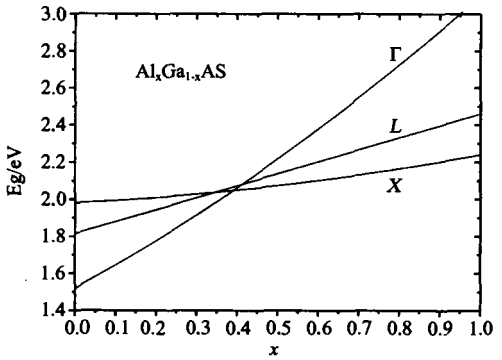

Fig. 4 Γ-, L- and X-valley energy gaps E_g versus $Al_xGa_{1-x}As$ compositionx. The bandgap structure parameters[10] and bowing parameters[11] used here are listed in Table 1

图4 $Al_xGa_{1-x}As$ 材料的Γ、L、和X能谷的带隙 E_g 随组分x的变化. 其中所使用的能带结构参数[10]和弯曲系数[11]列于表1中

The valley point in electron concentration is in agreement with the critical AlAs composition of direct-indirect crossover for Γ-X in the $Al_xGa_{1-x}As$ system. A quite similar phenomenon has been reported by Li et al. [12] in the Te doped n-AlGaAsSb system, where the Te incorporation was also dependent on the band structure of AlGaAsSb distinctly. The Hall electron mobility decreases almost linearly for $x < 0.4$, as predicted by theoretical calculations based on a shifted Maxwellian approach[13] and a Monte Carlo technique[14] for the three-valley conduction band model. For $x > 0.4$, the majority of electrons are in X valley, in which the transport is dominated by larger electron effective mass.

3 Conclusions

With a constant Si dopant temperature, more than 50 samples of $Al_xGa_{1-x}As$ were grown by GSMBE in an entire AlAs mole fraction for on a donor incorporation study. Accurate alloy compositions were obtained by the X-ray measurements, which also indicated excellent quality of epilayers. The electron concentrations exhibit strong dependence on the alloy composition of AlGaAs with the minimum at about $x = 0.4$ near the Γ-X direct-indirect band crossover. The Hall electron mobility shows nearly linear dependence on AlAs mole fraction for $x < 0.4$, and remains low and only varies a little for higher x.

REFERENCES

[1] Ishibashi T, Tarucha S, Okamoto H. Si and Sn Doping in $Al_xGa_{1-x}As$ Grown by MBE[J]. *Jpn. J. Appl. Phys.*, 1982, **21**: L476—L478.

[2] Ishikawa T, Saito J, Sasa S, *et al.* Electrical properties of Si-Doped $Al_xGa_{1-x}As$ layers grown by MBE[J]. *Jpn. J. Appl. Phys.*, 1982, **21**: L675—L676.

[3] Chand N, Henderson T, Klem J, *et al.* Comprehensive analysis of Si-doped $Al_xGa_{1-x}As$ ($x = 0$ to 1): Theory and experiments[J]. *Phys. Rev. B*, 1984, **30**: 4481—4492.

[4] Lang D V, Logan R A, Jaros M. Trapping characteristics and a donor-complex (*DX*) model for the persistent-photoconductivity trapping center in Te-doped $Al_xGa_{1-x}As$[J]. *Phys. Rev. B*, 1979, **19**: 1015—1030.

[5] XIAO Xi-Feng, KANG Jun-Yong. Two DX-Like centers in Sn-doped AlGaAs alloy semiconductors[J]. *J. Infrared Millim. Waves*(肖细凤,康俊勇,AlGaAs:Sn混晶中的两类DX中心,红外与毫米波学报),2002, **21** suppl: 83—86.

(下转9页)

[3] Kim J D, Kim S, Wu D, *et al.* 8 ~ 13μm InAsSb heterojunction photodiode operating at near room temperature [J]. *Appl. Phys. Lett.* 1995, **67**(18): 2645—2647.

[4] LI Guo-Hua, CHEN Ye, FANG Zai-Li, *et al.* Photoluminescence of low-dimensional semiconductor structures under pressure [J]. *J. Infrared Millim. Maves*(李国华,陈晔,方再利,等. 半导体低维结构的压力光谱研究. **红外与毫米波学报**),2005,**24**(3):174—178.

[5] Hung W K, Chern M Y, Chen Y F, *et al.* Optical properties of $GaAs_{1-x}N_x$ on GaAs [J]. *Phys. Rev. B*, 2000, **62**(19): 13028—13033.

[6] Aspnes D E, Studna A A. Dielectric functions and optical parameters of Si, Ge, GaP, GaAs, GaSb, InP, InAs, and InSb from 1.5 to 6.0 Ev [J]. *Phys. Rev. B*, 1983, **27**(2): 985—1009.

[7] Deng H Y, Dai N. High-lying interband transitions and optical properties of $InAs_{1-x}Sb_x$ films [J]. *Phys. Rev. B*, 2006, **73**: 113102.

[8] Adachi S. Model dielectric constants of GaP, GaAs, GaSb, InP, InAs, and InSb [J]. *Phys. Rev. B*, 1987, **35**(14): 7454—7463.

[9] Adachi S. Optical properties of $Al_xGa_{1-x}As$ alloys [J]. *Phys. Rev. B*, 1988, **38**(17): 12345—12352.

[10] Brust D, Phillips J C, Bassani F. Critical points and ultraviolet reflectivity of semiconductors [J]. *Phys. Rev. Lett.* 1962, **9**(3): 94—97.

(上接 4 页)

[6] Watanabe M O, Morizuka K, Mashita M, *et al.* Donor levels in Si-Doped AlGaAs grown by MBE[J]. *Jpn. J. Appl. Phys.*, 1984 **23**: L103—L105.

[7] Watanabe M O, Maeda H. Electron activation energy in Si-Doped AlGaAs grown by MBE[J]. *Jpn. J. Appl. Phys.*, 1984, **23**: L734—L736.

[8] ZHANG Yong-gang, GU Yi, ZHU Cheng, *et al.* Fabrication of short wavelength infrared InGaAs/InP photovoltaic detector series[J]. *J. Infrared Millm. Waves*(张永刚,顾溢,朱诚,郝国强,等. 短波红外 InGaAs/InP 光伏探测器系列的研制. **红外与毫米波学报**),2006, **25**(1), 6—9.

[9] HAO Guo-qiang, ZHANG Yong-gang, GU Yi, *et al.* Performance analysis of extended wavelength InGaAs photovoltaic detectors grown with gas source MBE[J]. *J. Infrared Millim. Waves*(郝国强,张永刚,顾溢,等,气态源分子束外延生长扩展波长 InGaAs 探测器性能分析. **红外与毫米波学报**),2006, **25**(4), 241—245.

[10] Vurgaftman I, Meyer J R, Ram-Mohan L R. Band parameters for Ⅲ - Ⅴ compound semiconductors and their alloys [J]. *J. Appl. Phys.*, 2001, **89**: 5815—5875.

[11] Levinshtein M, Rumyantsev S, Shur M. *Handbook Series on Semiconductor Parameters*[M]. Vol. 2 Singapore: World Scientific, 1999, Chap. 1, 5.

[12] Li A Z, Wang J X, Zheng Y L, *et al.* The behavior of dopant incorporation and internal strain in $Al_xGa_{1-x}As_{0.03}Sb_{0.97}$ grown by molecular beam epitaxy[J]. *J. Crystal Growth*, 1993, **127**: 566—569.

[13] Hava S, Auslender M. Velocity-field relation in GaAlAs versus alloy composition[J]. *J. Appl. Phys.*, 1993, **73**: 7431—7434.

[14] El-Ela F M A. Monte carlo simulation of electron transport in AlGaAs[J]. *AIP Conference Proceedings*, 2005, **748**: 86—92.